

Specific absorption rate distribution evaluation in a different substrate for hyperthermia treatment

Bibi Sarpinah Sh Naimullah^{1,2}, Kasumawati Lias¹, Norlida Buniyamin³, Ahmad Tirmizi Jobli⁴,
Mazlina Mansor Hassan^{1,2}

¹Faculty of Engineering, Universiti Malaysia Sarawak (UNIMAS), Samarahan, Malaysia

²School of Electrical Engineering, College of Engineering, Universiti Teknologi MARA (UiTM), Samarahan, Malaysia

³School of Electrical Engineering, College of Engineering, Universiti Teknologi MARA (UiTM), Shah Alam, Malaysia

⁴Faculty of Medical and Health Science, Universiti Malaysia Sarawak (UNIMAS), Samarahan, Malaysia

Article Info

Article history:

Received Jan 11, 2022

Revised Jun 9, 2022

Accepted Jul 7, 2022

Keywords:

Focus position distance

Hyperthermia

Microstrip antenna

Specific absorption rate

Substrate

ABSTRACT

Hyperthermia treatment procedure (HTP) is a treatment that uses high heat generated from electromagnetic (EM) waves, which is about 42 °C to 45 °C within a particular duration. However, poor focus position distance on the treated tissue has become a significant concern among the researchers since it may contribute to a wide area of unwanted hot spots, which lead to severe adverse health effects on healthy tissue. This paper presents a specific absorption rate (SAR) distribution evaluation of different microstrip antenna substrates with different electrical permittivities, contributing to different sizes of microstrip antenna patches, which then provide different attainment of the SAR distribution on the treated tissue. Operating frequencies of 434 MHz, 915 MHz, and 2,450 MHz with 10 W operating power are utilized. A SEMCAD X is used to conduct a simulation in obtaining the SAR distribution, which determines the focus position distance on different tumour (malignant tissue) sizes. Based on the results, the suitable substrate for frequency 915 MHz and 2,450 MHz is RT5880, and RT5870, while RO3210 and RT6010 performed their best at 434 MHz and 2,450 MHz. The finding of this study can be used for further research in optimizing microstrip antenna development for HTP.

This is an open access article under the [CC BY-SA](https://creativecommons.org/licenses/by-sa/4.0/) license.



Corresponding Author:

Bibi Sarpinah Sh Naimullah

Faculty of Engineering, Universiti Malaysia Sarawak (UNIMAS)

Samarahan 94300, Sarawak, Malaysia

Email: sarpinah187@gmail.com

1. INTRODUCTION

Hyperthermia treatment procedure (HTP) is a treatment procedure that utilizes high heat, about 42 °C to 45 °C at a certain period, to denature cancer cells into necrotic tissue with minimal damage to surrounding healthy tissue [1], [2]. The HTP provides non-invasive and invasive techniques. The non-invasive, which is referred to as treatment, is placing an applicator on the skin. On the other hand, invasive treatment is a procedure where the applicator is inserted into the target tissue. The treatment procedure can be hyperthermia alone or a combination of radiotherapy/chemotherapy. This paper focuses on non-invasive hyperthermia techniques for breast cancer treatment, which works alone by using the microstrip antenna as a hyperthermia heat applicator.

Hyperthermia is safer if compared to other currently available treatments for cancer. However, the main concern of this hyperthermia treatment is the focusing heat on the treated tissue [3]-[10]. The

electromagnetic (EM) technique is used as the heating source. The microstrip antenna or an applicator transfer the EM wave to the target tissue. The breast cancer stage is based on tumour size and categorized from T1 to T4. This research cover T1 to T3 only.

Meanwhile, T4 involves cell cancer spreading to other areas such as the chest wall or skin [11]. A tumour is said to be benign or malignant tissue. Benign tissue is non-cancerous, while malignant tissue is cancerous [12]. Therefore, in this research, tumours refer to malignant tissue that is confirmed with cancerous tissue analyzed.

Effective hyperthermia treatment means high absorption in the malignant tissue and low power absorbed in healthy tissue. In order to ensure high heat absorption into the targeted cancer tissue, the main part that needs to take into account is the hyperthermia applicator. The type, structure, shape, and characteristics of the designed hyperthermia applicators may influence the capacity of heat to be absorbed by the targeted treated cancer tissue. In conjunction with that, in this paper, the microstrip antenna performance as the hyperthermia applicator that contributes to the effectiveness of HTP [13], [14] is investigated. Since the heat absorption into the cancer tissue is affected by the permittivity properties of the cancer tissue and hyperthermia applicator, hence this research is carried out to observe the effects of different microstrip substrates on the heat distribution into the treated cancer tissue.

The performances of nine different substrates towards specific absorption rate (SAR) distribution are investigated. The substrate used is RT5880, RT5870, RT6010, RO4003C, RO3003, RO3210, RO3010, FR4, and F4B. These are the common substrate used in the microstrip antenna based on the previous study. The most preferable is FR4 [15]-[18], then follow with RT5880 [19]-[21], RO4003C [22], [23] and F4B. The others substrate such as F4B [24], RO5870 [25], RT 6010 [26], RO3003, RO3010 [27], and RO3210 are used with less preferable.

Both RT/Duroid 5870 and 5880 are glass microfiber reinforced polytetrafluoroethylene (PTFE) composites, while RT6010 laminates are ceramic PTFE composites, with relative permittivity of 2.33, 2.20, and 10.7, respectively. The RO4003C with relative permittivity of 3.55 is glass-reinforced hydrocarbon/ceramic laminates. Meanwhile, RO3003 with relative permittivity 3.0 is described as a laminate ceramic-filled PTFE composite. Although the relative permittivity for RO3010 and RO3210 is the same, 10.2, the laminated material is different. The RO3010 laminated ceramic filled PTFE composites while RO3210 laminates ceramic filled with woven fiberglass. Meanwhile, FR4 is a glass epoxy laminated material with relative permittivity of 4.4. It is a less costly material. F4B is mainly PTFE glass fiber cloth and ceramic-filled PTFE glass fiber cloth with relative permittivity of 2.65.

This paper compares the performance of each substrate by analyzing the specific absorption rate (SAR) distribution. SAR is defined as the rate of energy absorbed in the treated tissue. Therefore, the suitable substrate is selected based on the SAR evaluation and meets the desired focus position distance (FPD). Desired FPD is the measurement based on the mammogram breast cancer analysis. Another significant result that needs to be considered is operating frequency suitable in T1, T2, and T3. The following section describes the methodology.

2. RESEARCH METHOD

Research methodology is divided into three main parts. The first part is phantom breast development, the second is malignant tissue development, and the third is rectangular microstrip development. The development of each part is elaborated in the following sections; subsections 2.1 to 2.2.

2.1. Malignant tissue development

The research begins with the initial step, where the analysis of 149 mammogram malignant images. The mammogram images are analyzed with digital imaging and communications in medicine (DICOM) to obtain the actual focus position distance (FPD) measurement. The images can be divided into two common positioning views: Medio-lateral oblique (MLO) and Cranio-Caudal (CC), used for breast cancer detection and diagnosis [28]. The data extracted from the analysis are surface and inner depth distances. Surface depth is a measurement of the mamilla to the first point of malignant tissue. In comparison, the inner depth is the measurement of the mamilla to the last end of malignant tissue [29].

The mammogram image is analyzed based on tumour/malignant tissue size. T is referred to as a tumour, and there are T1 to T3 categories [30]. Therefore, the data are then categorized into T1, T2, and T3. T1 is defined as a tumour size/diameter less than or equal to 20 mm ($T1 \leq 20$ mm). While $20 \text{ mm} < T2 \leq 50$ mm and $T3 > 50$ mm [11]. The average surface and inner depth in both views, MLO and CC, are determined. Next, the surface depth and inner depth are obtained. The value of surface depth and inner depth for T1, T2, and T3 in Table 1. The surface depth, inner depth, and diameter of malignant tissue are determined by (1)-(5).

Table 1. Surface depth and inner depth

	T1	T2	T3
Surface depth(mm)	50	48	28
Inner depth(mm)	64	80	90
Diameter(mm)	14	32	62

$$\text{Average MLO / CC Surface depth, } \bar{S} = \frac{\sum_{i=1}^N x_i}{N} \tag{1}$$

$$\text{Average MLO /CC Inner depth, } \bar{I} = \frac{\sum_{i=1}^N x_i}{N} \tag{2}$$

where N=number of a set of data

x_i = sum of x value $(\frac{x_1 + x_2 + x_3 + x_4 + \dots + x_N}{N})$

$i= 1,2,3,4, \dots, N$

Hence, the surface depth and inner depth are determined based on (3)-(5).

$$\text{Surface depth, } S = \frac{\bar{S}_{MLO} + \bar{S}_{CC}}{2} \tag{3}$$

$$\text{Inner depth, } I = \frac{\bar{I}_{MLO} + \bar{I}_{CC}}{2} \tag{4}$$

$$\text{Diameter} = \text{Inner depth} - \text{surface depth} = S - I \tag{5}$$

SEMCAD X 14.8.4 is used to model the phantom breast, malignant tissue, and rectangular microstrip. The malignant tissue is developed based on (5). Hence, the malignant tissue is constructed into three categories, T1 to T3. Three different frequencies are used in this experiment simulation. Further explanation of the microstrip model is provided in subsection 2.2

2.2. Rectangular microstrip development

The rectangular microstrip antenna is designed with nine different substrates with a 1mm thickness. The results are observed on each substrate mm with operation power, Pin 10W. Specific absorption rate (SAR) on each 1g is observed for a 1-hour time duration. The dimension of the rectangular microstrip antennas is indicated in Tables 2-4 for different operating frequencies and substrates. The rectangular microstrip is designed and developed based on:

- a. Determine the patch width (W)

$$W = \frac{c}{2f_r} \sqrt{\frac{2}{\epsilon_r + 1}}$$

where f = operational frequency, ϵ_r =substrate permittivity, and c is the speed of EM wave in vacuum= $3 \times 10^8 \text{ms}^{-1}$

- b. Find the effective dielectric constant (ϵ_{reff})

$$\epsilon_{\text{reff}} = \frac{\epsilon_r + 1}{2} + \frac{\epsilon_r - 1}{2} \left[\frac{1}{\sqrt{1 + \frac{12h}{W}}} \right]$$

where h = substrate thickness

- c. Compute the effective Length (L_{eff}). The typical values of the characteristic impedance are either 50Ω or 75Ω. In this research, the transmission line of 50Ω is used.

$$L_{\text{eff}} = \frac{c}{2f_r \sqrt{\epsilon_{\text{reff}}}}$$

- d. Calculate the patch extensin (ΔL)

$$\Delta L = 0.412h \frac{(\epsilon_{\text{reff}} + 0.3) \left(\frac{W}{h} + 0.264\right)}{(\epsilon_{\text{reff}} - 0.258) \left(\frac{W}{h} + 0.8\right)}$$

ΔL is extension length due to the fringing effect where the EM waves expand to the outside patch.

- e. Determine the actual patch length (L)

$$L_{\text{eff}} = L + 2\Delta L$$

$$L = L_{\text{eff}} - 2\Delta L$$

- f. Calculation of ground plane dimensions

Length of the ground plane (L_g) and width of the ground plane (W_g):

$$L_g = L + 6h$$

$$W_g = W + 6h$$

Table 2. Dimension of rectangular microstrip antenna $f=434$ MHz

434 MHz				
Substrate	W_g (mm)	L_g (mm)	W_{copper} (mm)	L_{copper} (mm)
F4B	261.664	217.904	255.664	211.904
FR4	224.439	178.606	218.439	172.605
RO3003	250.223	205.208	244.222	199.208
RO3010	145.841	109.3	139.842	103.3
RO3210	151.951	114.233	145.951	108.233
RO4003C	234.987	189.183	228.987	183.183
RT Duroid 6010	148.192	111.191	142.192	105.191
RT5870	273.666	231.926	267.666	225.926
RT5880	279.049	238.475	273.049	232.475

Table 3. Dimension of rectangular microstrip antenna $f=915$ MHz

915 MHz				
Substrate	W_g (mm)	L_g (mm)	W_{copper} (mm)	L_{copper} (mm)
F4B	127.266	106.349	121.266	100.3494
FR4	109.610	87.797	103.610	81.7972
RO3003	121.839	100.359	115.839	94.3593
RO3010	72.329	55.004	66.329	49.004
RO3210	75.227	57.341	69.227	51.3413
RO4003C	114.612	92.794	108.612	43.3968
RT Duroid 6010	73.444	55.900	67.444	49.900
RT5870	132.959	112.961	126.959	106.9607
RT5880	135.512	116.047	129.512	110.0471

Table 4. Dimension of rectangular microstrip antenna $f=2450$ MHz

2,450 MHz				
Substrate	W_g (mm)	L_g (mm)	W_{copper} (mm)	L_{copper} (mm)
F4B	51.289	43.238	45.289	37.238
FR4	44.695	36.402	38.695	30.402
RO3003	49.262	41.035	43.262	35.035
RO3010	30.772	24.225	24.772	18.225
RO3210	31.854	25.097	25.854	19.097
RO4003C	46.563	38.247	40.563	32.247
RT Duroid 6010	31.188	24.559	25.188	18.559
RT5870	53.415	45.664	47.415	39.664
RT5880	54.369	46.795	48.369	40.795

The substrate listed in Tables 2 to 4 is used for microstrip design in SEMCAD X. The SAR distribution performance is observed, and the preferable substrate is the one that achieved desired FPD or nearly achieved FPD. This paper observation is only on FPD, and the SAR volume is not included. The FPD has surface depth (begin FPD) and inner depth (end FPD). The FPD that needs to be determined is desired FPD and measured FPD. This desired FPD was obtained based on the breast mammogram analysis indicated in Table 1. The measure of FPD is from SAR distribution results in SEMCAD X. The significance of selecting a suitable substrate is to ensure successful hyperthermia treatment. The success of HTP depends on the heat distributed to the malignant tissue and on avoiding/minimizing heat on the healthy tissue. Figure 1 shows the modeling development of breast phantom, malignant tissue, and microstrip on selected substrate RT6010 for frequency 434 MHz, while RT5880 for frequency 915 MHz and 2,450 MHz. The size of malignant (T1 to T3) was obtained based on (5). The breast phantom size is fixed for all conditions in T1 to T3.

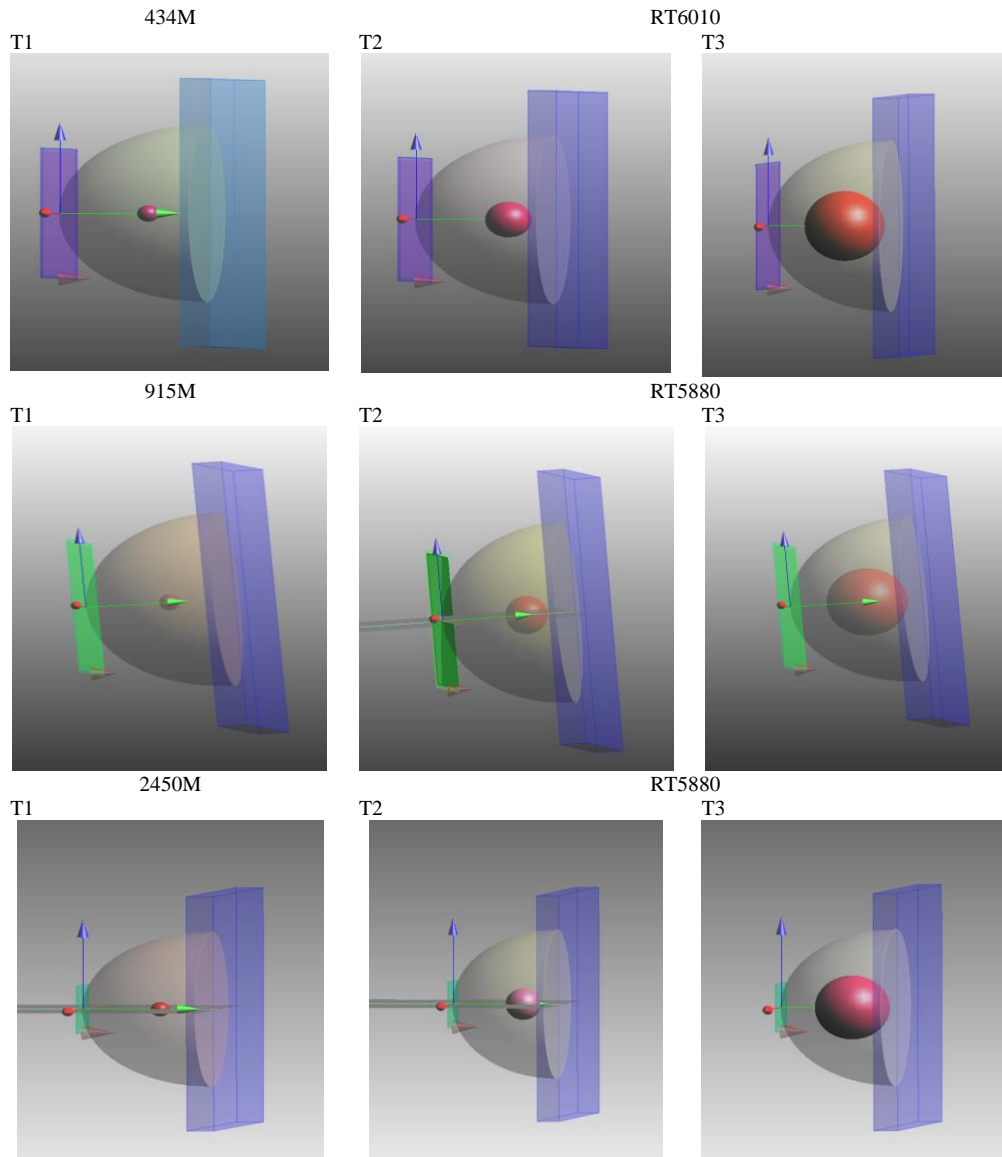


Figure 1. Breast phantom, malignant tissue modeling T1, T2.T3 in 434 MH, 915 MHz, and 2450 MHz with SEMCAD X

3. RESULTS AND DISCUSSION

The performance comparison of different substrates in the microstrip antenna for the HTP. The results are observed in SAR distribution results. The operation power, P_{in} , is set to 10W within a 1-hour time duration [31], and the temperature applies 45 °C [32]. Effects of SAR on each 1 g and investigated under 10 W means the rate of energy absorbed in the treated tissue. The SAR stated in (6). The heat-specific capacity is set to 3,510 J/kg °C [33].

$$SAR = \frac{c\Delta T}{\Delta t} \Big|_{t=0} \tag{6}$$

where ΔT = change in temperature (°C)

Δt = the duration of exposure (s)

C= the specific heat capacity (J/kg °C)

The unit of SAR is stated as W/kg or mW/g

The results of FPD for RO3210 and RT6010 are recorded in Tables 5 and 6, respectively. The frequencies 434 MHz and 2,450 MHz were selected based on SAR distribution. However, for RT5880 and RT5870, the preferable frequencies are 915 MHz and 2,450 MHz. It is shown that RT5880 and RT5870

attained FPD in T1, whereas in T2 and T3, the results reached the beginning FPD. The FPD in RT5880 is -0.9 mm to 65.7 mm, -0.9 mm to 65.3 mm, and -0.9 mm to 50 mm for T1, T2, and T3 as in Table 7. Similar to RT5870, the FPD is -0.852 mm to 65.6 mm, -0.85 to 65.3 mm, -0.88 to 49.6 mm for T1, T2, and T3, respectively as shown in Table 8.

At the frequency 434 MHz, microstrip antenna design with substrates RT5880, RT5870, F4B, RO3003, RO4003C and FR4 are evaluated. The SAR distribution results show no heating on these substrates in all tumor sizes, T1 to T3. However, the SAR distribution shows the heating distribution for the substrate RO3210 and RT6010 in T1 to T3, as depicted in Table 5 and Table 6. In particular, RO3010 results show no heating in SAR distribution for T1. Nevertheless, there is heating in the SAR distribution of T2 and T3 for RO3010. Measure FPD is 11.8 mm to 19.3 mm in T2 and 11.5 mm to 19 mm in T3, which is considered far from the desired FPD compared to RO3210 and RT6010. Desired FPD is determined based on the breast mammogram image analysis, as listed in Table 1. Meanwhile, in T3, RO3210, and RT6010, the SAR distribution meets the begin FPD; begin FPD refers to the first point of malignant tissue (surface depth). Therefore, the preferable substrate frequency 434 MHz in T1 to T3 are RO3210 and RT6010.

At frequency 915 MHz, and 2,450 MHz, all substrate shows the SAR distribution has the heating process. Nevertheless, the best substrate that nearly achieved desired FPD or achieved desired FPD is RT5880 and RT5870. In 915 MHz, RT5880 has FPD 11.6 mm to 29.5 mm, 12.3 mm to 26.5 mm, and 12.3 mm to 30.5 mm for T1, T2, and T3, respectively, as indicated in Table 7. Similar to 2,450 MHz, the RT5880 and RT5870 are the appropriate substrates based on SAR distribution. Furthermore, RT5880 and RT5870 attained FPD in T1, whereas in T2 and T3, the results reached the beginning FPD. The FPD in RT5880 is -0.9 mm to 65.7 mm, -0.9 mm to 65.3 mm, and -0.9 mm to 50 mm for T1, T2, and T3, as in Table 7. Similar to RT5870, the FPD is -0.852 mm to 65.6 mm, -0.85 to 65.3 mm, and -0.88 to 49.6 mm for T1, T2, and T3, respectively, as represented in Table 8.

Table 5. FPD based on SAR distribution with frequency 434 MHz and 2,450 MHz in T1, T2, and T3

	434 MHz RO3210	2450 M RO3210
T1	FPD=16.7 mm to 19.8 mm	FPD=-0.9 mm to 60.2 mm
T2	FPD=21.6 mm to 23.3 mm	FPD=-0.916 mm to 57.6 mm
T3	FPD=19.7 mm to 25 mm	FPD=-0.91 mm to 46.3 mm

Table 6. FPD based on SAR distribution with frequency 434 MHz and 2,450 MHz in T1, T2, and T3

	434 MHz RT6010	2450 M RT6010
T1	FPD=11.2 mm to 24.8 mm	FPD=-0.94 mm to 60.6 mm
T2	FPD=11.3 mm to 24.5 mm	FPD=-0.94 mm to 58.5 mm
T3	FPD=19.4 mm to 26 mm	FPD=-0.93 mm to 46.8 mm

It can be seen the low-frequency 434 MHz is more compatible with high relative permittivity. Indeed, RO3210 and RT6010 have a high dielectric value of 10.2 and 10.8, respectively. In contrast to frequency 915 MHz, the relative permittivity for RT5880 is 2.2, while 2.33 for RT5870. Both have low dielectric values. All the substrates are acceptable in frequency 2450 MHz, but then subtract that nearly achieved FPD are RT5880, RT5870, F4B, RO3003, and RO4003C. These substrates have low dielectric values. Based on $w = \frac{c}{2f_r \sqrt{\epsilon_r + 1}}$, it can be rearranged as $f_r = \frac{c}{2w \sqrt{\epsilon_r + 1}}$. Hence, the frequency is inversely proportional to the under root of relative permittivity of the substrate. Thakur *et al.* [34] has explored the relationship of relative permittivity with bandwidth. The relative permittivity increases the bandwidth decrease.

The next section of the analysis is concerned with combination frequency 434 MHz, 915 MHz, 2,450 MHz, and combination 434 MHz and 915 MHz, and the results show no suitable common substrate proposed. Further analysis shows that combination frequency with a common substrate is found in 434 MHz, 2,450 MHz, and 915 MHz, 2,450 MHz. Thus the proposed substrate for combination frequency 434 M and 2450 M are RO3210 and RT6010. Likewise, proposed common substrates for combination frequency 915 M and 2,450 M are RT5880 and RT5870.

FR4 is the preferred substrate used in microstrip design since it is a less expensive material [35]. However, based on this study, it looks like FR4 is not preferable in HTP. Moreover, the microstrip antenna substrate FR4 at frequencies 434 MHz and 915 MHz shows no heating in the SAR distribution. Previous studies [35]–[37] have reported that RT Duroid shows a better radiation pattern, gain, and directivity than

other substrates. Therefore the proposed substrate is RT5880, RT5870 for frequency 915 M and 2,450 MHz, while RO3210, RT6010 for 434 MHz and 2,450 MHz.

Table 7. FPD based on SAR distribution with frequency 915 MHz and 2,450 MHz in T1, T2, and T3

	915 MHz RT5880	2450 M RT5880
T1	FPD=11.6 mm to 29.5 mm	FPD=-0.9 mm to 65.7 mm
T2	FPD=12.3 mm to 26.5 mm	FPD=-0.9 mm to 65.3 mm
T3	FPD=12.3 mm to 30.5 mm	FPD=-0.9 mm to 50 mm

Table 8. FPD based on SAR distribution with frequency 915 MHz and 2,450 MHz in T1, T2, and T3

	915 MHz RT5870	2450 M RT5870
T1	FPD=12 mm to 29.4 mm	FPD=-0.852 mm to 65.6 mm
T2	FPD=12.6 mm to 26.9 mm	FPD=-0.85 mm to 65.3 mm
T3	FPD=12.6 mm to 29.6 mm	FPD=-0.88 mm to 49.6 mm

4. CONCLUSION

Nine substrate, RT5880, RT5870, RT6010, RO4003C, RO3003, RO3210, RO3010, FR4, and F4B. Used as substrate in microstrip antenna design and simulated with SEMCAD X to obtain SAR distribution. FPD measurement is based on the SAR distribution obtained in SEMCAD X. The desired FPD is determined from mammogram breast cancer analysis. The study proposed preference subtract for frequency 434 MHz, 915 MHz, 2,450 MHz and also a common substrate for frequency combination such as 434 MHz, 2,450 MHz and 915 MHz, 2,450 MHz that is suited for HTP applications. The finding of this study can be used in further research in microstrip antenna development.

ACKNOWLEDGEMENTS

The author would like to thank Universiti Malaysia Sarawak (UNIMAS) for supporting this research under Cross-Disciplinary Research Grant, F02/CDRG/1840/2019. The author also would like to thank the College of Engineering, UiTM Sarawak, for their continuous support throughout this research.




REFERENCES

- [1] P. R. Stauffer, "Evolving technology for thermal therapy of cancer," *International Journal of Hyperthermia*, vol. 21, no. 8, pp. 731–744, Dec. 2005, doi: 10.1080/02656730500331868.
- [2] Y. S. Koo, R. Kazemi, Q. Liu, J. C. Phillips, and A. E. Fathy, "Development of a high SAR conformal antenna for hyperthermia tumors treatment," *IEEE Transactions on Antennas and Propagation*, vol. 62, no. 11, pp. 5830–5840, Nov. 2014, doi: 10.1109/TAP.2014.2357419.
- [3] I. Elshafey, A.-F. Sheta, M. A. N. Uddin, W. M. Abdulkawi, and W. A. Malik, "Adaptive energy concentration in hyperthermia treatment of cancer," in *2019 IEEE Asia-Pacific Conference on Applied Electromagnetics (APACE)*, Nov. 2019, pp. 1–5, doi: 10.1109/APACE47377.2019.9021009.
- [4] H. F. G. Mendez, M. A. P. Arango, F. C. Rico, and I. E. D. Pardo, "Microwave hyperthermia study in breast cancer treatment," in *2019 Congreso Internacional de Innovación y Tendencias en Ingeniería (CONIITI)*, Oct. 2019, pp. 1–5, doi: 10.1109/CONIITI48476.2019.8960873.
- [5] P. R. Stauffer, "Designing effective microwave antennas for clinical applications in thermal medicine," in *Proceedings of European Microwave Conference in Central Europe, EuMCE 2019*, 2019, pp. 403–408.
- [6] H. F. G. Mendez, M. A. P. Arango, J. J. P. Acosta, J. F. C. Rico, and J. S. A. Opayome, "Hyperthermia study in breast cancer treatment using three applicators," in *Communications in Computer and Information Science*, vol. 1052, 2019, pp. 416–427.
- [7] J. Li and X. Wang, "Comparison of Two small circularly polarized antennas for focused microwave hyperthermia," in *13th European Conference on Antennas and Propagation, EuCAP 2019*, 2019.
- [8] N. A. Jaffar, K. B. Lias, N. K. Madzhi, and N. Buniyamin, "An overview of metamaterials used in applicators in hyperthermia cancer treatment procedure," in *2017 International Conference on Electrical, Electronics and System Engineering (ICEESE)*, Nov. 2017, vol. 2018-Janua, pp. 32–36, doi: 10.1109/ICEESE.2017.8298389.
- [9] D. A. M. Iero, L. Crocco, T. Isernia, and E. Korkmaz, "Optimal focused electromagnetic hyperthermia treatment of breast cancer," in *2016 10th European Conference on Antennas and Propagation (EuCAP)*, Apr. 2016, pp. 1–2, doi: 10.1109/EuCAP.2016.7481515.
- [10] K. Lias, N. Buniyamin, and M. Z. A. Narihan, "Specific Absorption rate investigation of different EBG-M applicator structures for non-invasive hyperthermia cancer treatment procedure," in *IFMBE Proceedings*, vol. 56, 2016, pp. 103–106, doi: 10.1007/978-981-10-0266-3_21.
- [11] J. Koh and M. J. Kim, "Introduction of a new staging system of breast cancer for radiologists: an emphasis on the prognostic stage," *Korean Journal of Radiology*, vol. 20, no. 1, p. 69, 2019, doi: 10.3348/kjr.2018.0231.
- [12] M. Z. A. Narihan, *A story of pathology and cancer*. UNIMAS, Kota Samarahan, Malaysia: UNIMAS, 2020.
- [13] M. B. Tayel, T. G. Abouelnaga, and A. Elnagar, "Dielectric loaded Yagi fed dual band pyramidal horn antenna for breast hyperthermia treatment," in *2018 5th International Conference on Electrical and Electronic Engineering (ICEEE)*, May 2018, pp. 323–328, doi: 10.1109/ICEEE2.2018.8391355.




- [14] E. Korkmaz, O. Isik, and H. Sagkol, "A directive antenna array applicator for focused electromagnetic hyperthermia treatment of breast cancer," in *2015 9th European Conference on Antennas and Propagation, EuCAP 2015*, 2015.
- [15] Z. Liang and J. Yuan, "Compact dual-wideband multi-mode printed quasi-Yagi antenna with dual-driven elements," *IET Microwaves, Antennas & Propagation*, vol. 14, no. 7, pp. 662–670, Jun. 2020, doi: 10.1049/iet-map.2019.0693.
- [16] O. W. Ata, M. Salamin, and K. Abusabha, "Double U-slot rectangular patch antenna for multiband applications," *Computers and Electrical Engineering*, vol. 84, p. 106608, Jun. 2020, doi: 10.1016/j.compeleceng.2020.106608.
- [17] J. Lin, H. Zhao, H. Lu, L. Geng, and T. Wang, "Generating the dual-band and multimode OAM by irregular pentagonal patch antenna array," *Electronics Letters*, vol. 56, no. 10, pp. 476–478, May 2020, doi: 10.1049/el.2020.0145.
- [18] L. Zhuo, H. Han, X. Shen, and H. Zhao, "A U-shaped wide-slot dual-band broadband NB-IoT antenna with a rectangular tuning stub," in *Proceedings of 2020 IEEE 4th Information Technology, Networking, Electronic and Automation Control Conference, ITNEC 2020*, Jun. 2020, pp. 123–128, doi: 10.1109/ITNEC48623.2020.9084751.
- [19] S. S. Chaudhury, S. Awasthi, and R. K. Singh, "Dual band bandpass filter based on substrate integrated waveguide loaded with mushroom resonators," *Microwave and Optical Technology Letters*, vol. 62, no. 6, pp. 2226–2235, Jun. 2020, doi: 10.1002/mop.32315.
- [20] G. Xu, H.-L. Peng, Z. Shao, L. Zhou, Y. Zhang, and W.-Y. Yin, "Dual-band differential shifted-feed microstrip grid array antenna with two parasitic patches," *IEEE Transactions on Antennas and Propagation*, vol. 68, no. 3, pp. 2434–2439, Mar. 2020, doi: 10.1109/TAP.2019.2943409.
- [21] P. Mathur and G. Kumar, "Dual-frequency dual-polarised shared-aperture microstrip antenna array with suppressed higher order modes," *IET Microwaves, Antennas & Propagation*, vol. 13, no. 9, pp. 1300–1305, Jul. 2019, doi: 10.1049/iet-map.2018.5442.
- [22] K. L. Chung, X. Yan, Y. Li, and Y. Li, "A Jia-shaped artistic patch antenna for dual-band circular polarization," *AEU - International Journal of Electronics and Communications*, vol. 120, p. 153207, Jun. 2020, doi: 10.1016/j.aeue.2020.153207.
- [23] B. Yin and Z. Lin, "A novel dual-band bandpass SIW filter loaded with modified dual-CSRRs and Z-shaped slot," *AEU - International Journal of Electronics and Communications*, vol. 121, p. 153261, Jul. 2020, doi: 10.1016/j.aeue.2020.153261.
- [24] J. Chen, Y. Zhao, Y. Ge, and L. Xing, "Dual-band high-gain fabry-perot cavity antenna with a shared-aperture FSS layer," *IET Microwaves, Antennas and Propagation*, vol. 12, no. 13, pp. 2007–2011, Oct. 2018, doi: 10.1049/iet-map.2018.5183.
- [25] S. Gao, L. Ge, D. Zhang, and W. Qin, "Low-profile dual-band stacked microstrip monopolar patch antenna for WLAN and car-to-car communications," *IEEE Access*, vol. 6, pp. 69575–69581, 2018, doi: 10.1109/ACCESS.2018.2877420.
- [26] N. Ganeshwaran, J. K. Jeyaprakash, M. G. N. Alsath, and V. Sathyanarayanan, "Design of a dual-band circular implantable antenna for biomedical applications," *IEEE Antennas and Wireless Propagation Letters*, vol. 19, no. 1, pp. 119–123, Jan. 2020, doi: 10.1109/LAWP.2019.2955140.
- [27] P. C. Aranibar, A. G. Lampérez, S. L. Romano, and D. S. Vargas, "Dual-band band-stop microstrip filter with controllable bands based on unequal split ring resonators," *IET Microwaves, Antennas and Propagation*, vol. 13, no. 12, pp. 2119–2128, Oct. 2019, doi: 10.1049/iet-map.2018.5926.
- [28] A. S. Ashour, *Springer tracts in nature-inspired computing applied nature-inspired computing: Algorithms and Case Studies*. Springer, 2020.
- [29] M. M. H. B. S. Naimullah, K. Lias, and N. Buniyamin, "An overview study of dual-band microstrip antenna for non-invasive hyperthermia treatment," *International Journal of Advanced Research in Engineering and Technology (IJARET)*, vol. 11, no. 8, pp. 738–746, 2020, doi: 10.34218/IJARET.11.8.2020.071.
- [30] L. Cong *et al.*, "Tumor size classification of the 8th edition of TNM staging system is superior to that of the 7th edition in predicting the survival outcome of pancreatic cancer patients after radical resection and adjuvant chemotherapy," *Scientific Reports*, vol. 8, no. 1, p. 10383, Dec. 2018, doi: 10.1038/s41598-018-28193-4.
- [31] C. C. Vernon and J. V. D. Zee, "Hyperthermia in cancer treatment," *Lancet*, vol. 345, no. 8965, pp. 1–48, 1995.
- [32] R. Habash, R. Bansal, D. Krewski, and H. T. Alhafid, "Thermal therapy, part 1: an introduction to thermal therapy," *Critical Reviews in Biomedical Engineering*, vol. 34, no. 6, pp. 459–489, 2006.
- [33] W. V. Ling, K. Lias, N. Buniyamin, H. M. Basri, and M. Z. A. Narihan, "SAR distribution of non-invasive hyperthermia with microstrip applicators on different breast cancer stages," *Indonesian Journal of Electrical Engineering and Computer Science*, vol. 22, no. 1, pp. 232–240, Apr. 2021, doi: 10.11591/ijeecs.v22.i1.pp232-240.
- [34] A. Thakur, M. Chauhan, and M. Kumar, "Effect of substrate relative dielectric constant on bandwidth characteristics of line feed rectangular patch antenna," *International Journal of Engineering Science Invention Research & Development*, vol. 1, no. X, pp. 391–396, 2015, [Online]. Available: www.ijesird.com.
- [35] I. Khan, G. D., R. Gunjal, and R. Rashmitha, "Review of MSP antenna design for various substrates," *SSRN Electronic Journal*, pp. 1–4, 2018, doi: 10.2139/ssrn.3230632.
- [36] R. Mishra, R. G. Mishra, R. K. Chaurasia, and A. K. Shrivastava, "Design and Analysis of micro strip patch antenna for wireless communication," *International Journal of Recent Trends in Engineering and Research*, vol. 3, no. 3, pp. 1–5, Apr. 2017, doi: 10.23883/IJRTER.CONF.20170331.001.BKAJT.
- [37] A. Khan and R. Nema, "Analysis of five different dielectric substrates on microstrip patch antenna," *International Journal of Computer Applications*, vol. 55, no. 14, pp. 40–47, Oct. 2012, doi: 10.5120/8826-2905.

BIOGRAPHIES OF AUTHORS






Bibi Sarpinah Sh Naimullah    graduated from Universiti Teknologi MARA with a Bachelor of Engineering with Hons. (Electrical) in November 1999. She received Master Science (Communications and Networking Engineering) from Universiti Putra Malaysia (UPM) in 2004. Currently, she is doing a Ph.D. in Electronic Engineering at Universiti Malaysia Sarawak (UNIMAS). She can be contacted at email: sarpinah187@gmail.com.






Ir. Dr. Kasumawati Lias    graduated from Universiti Malaysia Sarawak (UNIMAS) with a B.Eng (Hons) in Electronics (Telecommunication) Engineering. She obtained M.Eng in Electrical and Electronics (Telecommunication) Engineering at UTM, Johor. She received her Doctor of Philosophy in Biomedical Engineering from Universiti Teknologi MARA (UiTM), Shah Alam, Malaysia. Currently, she is a lecturer at the Department of Electrical and Electronic Engineering at the Faculty of Engineering, UNIMAS. She specializes in Hyperthermia for Cancer Treatment. She is registered with the Board of Engineers, Malaysia (BEM) and a member of the Institute of Engineers Malaysia, IEM, and IEEE Engineering in Medicine and Biology Society. She can be reached at email: lkasumwati@unimas.my.






Professor Ir. Dr. Norlida Buniyamin    graduated from the University of Adelaide, Australia, with a Bachelor Degree in Electrical and Electronic Engineering (Hons.). She was a Research Fellow with the Malaysian Institute of Microelectronic Systems (MIMOS) before joining University Teknologi MARA as a lecturer in 1988. She then obtained M.Sc. in Industrial Control System from the University of Salford, U.K, in 1993 and a Ph.D. in the area Knowledge Management for Manufacturing Enterprises in 2004 from the University of Manchester, Institute of Science and Technology (UMIST), U.K. She is now a Professor of Electrical Engineering at UiTM, a Fellow of the Institution of Engineers, Malaysia, and Hon Fellow of the ASEAN Federation of Engineering Organisation (AFEO). Her current research interest is Industrial Automation and Robotics, Biomedical Engineering, Knowledge Management, and Engineering Education. She can be contacted at email: nbuniyamin@uitm.edu.my.



Ass Prof. Dr. Ahmad Tirmizi bin Jobli    is an Associate Professor in the Radiology Department, Faculty of Medicine and Health Sciences, University Malaysia Sarawak. He received Medical Degree (M.D) from University Malaysia Sarawak in 2004 and Master in Medicine (Radiology) from University Kebangsaan Malaysia in 2011. Further subspecialty training in neuroradiology was carried out in 2014 at the Institute of Neurology, London. Actively doing neuroradiology-related cases in clinical works, especially brain tumour imaging, and proactively involved in the rheumatological research done in Sarawak General Hospital. He has publications in the area of neuroradiology and rheumatology. He is Co-supervising one Master student and one Ph.D. candidate. He is currently practicing in Sarawak General Hospital and teaching undergraduate students at University Malaysia Sarawak. He can be connected via email: jatirmizi@unimas.my.



Mazlina Mansor Hassan    is a senior lecturer at Universiti Teknologi MARA, UiTM Kampus Samarahan. She received her first degree in Electrical Engineering with honors at UiTM Shah Alam. Her Master is in Telecommunication and Information Engineering from UiTM Shah Alam. She is now pursuing a Ph.D. in Biomedical Engineering field in the Engineering Faculty at Universiti Malaysia Sarawak (UNIMAS). Her research interest is in biomedical engineering, antennas, and mobile communication. She has received a few grants such as RAGS and several “Dana Kecemerlangan” grants from UiTM Sarawak. She is involved in several innovative competitions such as Invention, Innovation and Design (IID) from UiTM Kota Samarahan, Malaysian Technology Expo (MTE) Kuala Lumpur, IID Shah Alam, IDEAS from Sarawak and UiTM Cawangan Perlis, and have won a few awards such as silvers and the bronze medals. She can be contacted through email: mazlina2206@gmail.com.